Astron. Astrophys. 170, 20–26 (1986)

ASTRONOMY AND ASTROPHYSICS

Giant radio galaxy 0503-286

L. Saripalli[1,2], Gopal-Krishna[1], W. Reich[3], and H. Kühr[4]

[1] Radio Astronomy Centre, Tata Institute of Fundamental Research, P.O. Box 1234, I.I.Sc. Campus, Bangalore-560 012, India
[2] Joint Astronomy Programme, Dept. of Physics, I.I.Sc., Bangalore-560 012, India
[3] Max-Planck Institut für Radioastronomie, Auf dem Hügel 69, D-5300 Bonn-1, Federal Republic of Germany
[4] Max-Planck Institut für Astronomie, Königstuhl, D-6900 Heidelberg-1 Federal Republic of Germany

Received January 21, accepted May 20, 1986

Summary. Discovery of a giant radio galaxy 0503-286 is reported, based on an ongoing search for such objects using the Ooty-Synthesis Radio Telescope at 327 MHz. We additionally present maps of the source made at 1.4 and 2.7 GHz using the 100-metre Effelsberg Radio Telescope. The source is identified with a 15-mag elliptical at a redshift $z = 0.038$ and has a classical double radio structure extending over 40 arcmin which corresponds to a linear size of 2.5 Mpc ($q_0 = 0$, $H_0 = 50\,\mathrm{km\,s^{-1}\,Mpc^{-1}}$). The pronounced asymmetry of its double structure is probably related to the asymmetric environmental conditions that seem to prevail around the parent galaxy. We also summarize and discuss some properties related to the radio structure of other known giant radio galaxies.

Key words: radio galaxies – double radio sources – galaxy clustering

1. Introduction

Among the many hundred radio galaxies whose radio maps are now available in literature, only about a dozen are known to have sizes exceeding 1.5 Mpc (taking $H_0 = 50\,\mathrm{km\,s^{-1}\,Mpc^{-1}}$ and $q_0 = 0$). Since lobes of such giant radio galaxies have probably penetrated beyond any circumgalactic halo associated with the parent galaxy, their evolution might follow a course substantially different from the lobes of most radio galaxies. At Ooty, a systematic search for giant radio galaxies in the declination range $-30°$ to $+18°$ is currently in progress, employing the Ooty Synthesis Radio Telescope (OSRT) described by Swarup (1984). The candidates were selected for radio mapping as follows: We first formed pairs of radio sources listed in the Molonglo Reference Catalogue (Large et al., 1981) on the criteria that at least one member of each pair is listed as an extended ($\gtrsim 1$ arcmin) or complex source and the separation between the pair is in the range 15–45 arcmin. We then examined the optical fields of these pairs using the Palomar-Sky-Survey prints and selected those cases where a bright elliptical ($\lesssim 17$ mag) was seen located roughly midway between the pair but not coinciding with each member of the pair. We are engaged in radio mapping of about 15 of the pairs selected in this manner. One of these pairs, reported here, is listed in the Molonglo catalogue as two individual sources, namely 0503-284 and 0503-290. An early OSRT map of this pair at 327 MHz revealed extensions of the two sources towards each other. Subsequent observations made in October 1984 using the 100-metre Effelsberg radio telescope at 1.4 GHz confirmed these extensions (Sect. 2). Thereafter we have mapped this source again at 327 MHz with OSRT during Feb. and Oct., 1985 and also at 2.7 GHz with the Effelsberg telescope during Sept., 1985. We have also obtained the optical spectrum of the parent elliptical galaxy, as discussed below.

Send offprint requests to: L. Saripalli

2. The radio observations

In Table 1 we summarise some observational details. The resultant maps at 327, 1420 and 2695 MHz are shown in Fig. 1. Since the source is extended in declination, the synthesis observations at 327 MHz were carried out after widening the field-of-view of OSRT. For this the largest element of the array (i.e., the Ooty radio telescope) was divided into ten equal parts, of which only the alternate 5 were actually used for observations, owing to the limited availability of correlators. This provided a primary beam of half-power width $\sim 3°$ (R.A.) $\times$ 1°3(dec.). The scatter of visibility data points was found to peak around 9 Jy. It may be noted that the shortest available spacing in the north-south direction is 90λ, due to which structures on scale $\gtrsim 15$ arcmin in declination are likely to have been significantly attenuated. Figure 1a shows a CLEANed map of the source at 327 MHz, restored with a gaussian beam of HPW = 3 arcmin. The contour values have been corrected for the attenuation caused by the OSRT primary beam. Another OSRT map with a higher resolution of 1.5 arcmin at 327 MHz is shown in Fig. 1b. The maps at 1420 and 2695 MHz made with the 100 m dish at Effelsberg are shown in Figs. 1c

Table 1. Observational parameters

Frequency	(MHz)	327	1420	2695
Telescope		OSRT	Effelsberg	Effelsberg
HPBW	(′)	3, 1.5	9.3	4.3
Calibrator		0519-208	3C 71	3C 286
Flux	(Jy)	8.5	5.1	10.4
Degree of pol.	(%)	–	–	9.9
Pol. angle	(°)	–	–	33

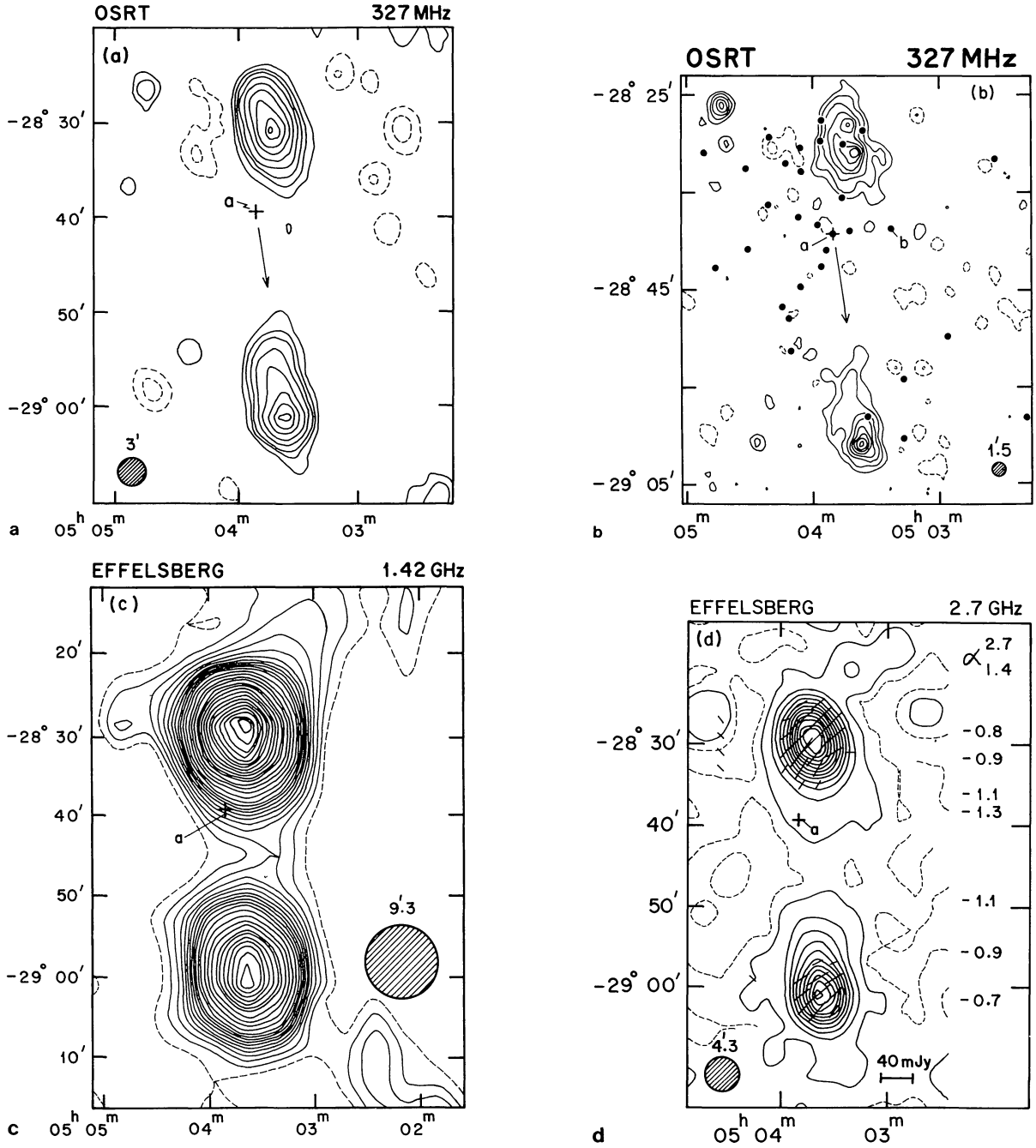

Fig. 1a-d. Total intensity maps of 0503-286 at 327, 1420 and 2695 MHz. Half-power beamwidths are represented by the shaded circles. The position of the parent galaxy 'a' is indicated on each map. The arrow marks the direction of the southern hot spot from the nucleus (see text). The 'plus' signs in **b** mark the positions of the galaxies seen on the Palomar-Sky-Survey prints (Sect. 5.1). In **d** are shown the E-vectors superimposed on total intensity contours, whose magnitudes are proportional to the linearly polarized flux, as defined by the horizontal bar. The vertical array of numbers on the right side displays the run of spectral index along the source axis which nearly coincides with a north-south line drawn at $\alpha = 05^h03^m39^s$. The contour levels for the 4 maps are: **a** (-1, -0.5, 0.5, 1, 1.5, 2.5, 4, 6, 8, 10 and 11) × 107 mJy, **b** (-0.5, -0.25, 0.25, 0.5, 1, 1.5, 2, 2.5, 3, 3.5) × 107 mJy, **c** 25 mJy upto the first 10 contours and 50 mJy thereafter, **d** 29 mJy

and 1d. The reduction of the Effelsberg data is based on the NOD2 map-making procedure (Haslam, 1974).

3. The optical observations

For reasons given in Sect. 4, we identify the source 0503-286 with the 15-mag D galaxy marked as 'a' in Fig. 1. The galaxy is centred at the following position, with an uncertainty of 2 arcsec in each coordinate:

$\alpha(1950) = 05^h03^m51^s.0$, $\delta(1950) = -28°39'19''$

Optical spectroscopy of this elliptical was carried out during the dark night of March 14, 1985 using the 2.2-metre telescope of the Max-Planck-Institut für Astronomie, at La Silla. The CCD

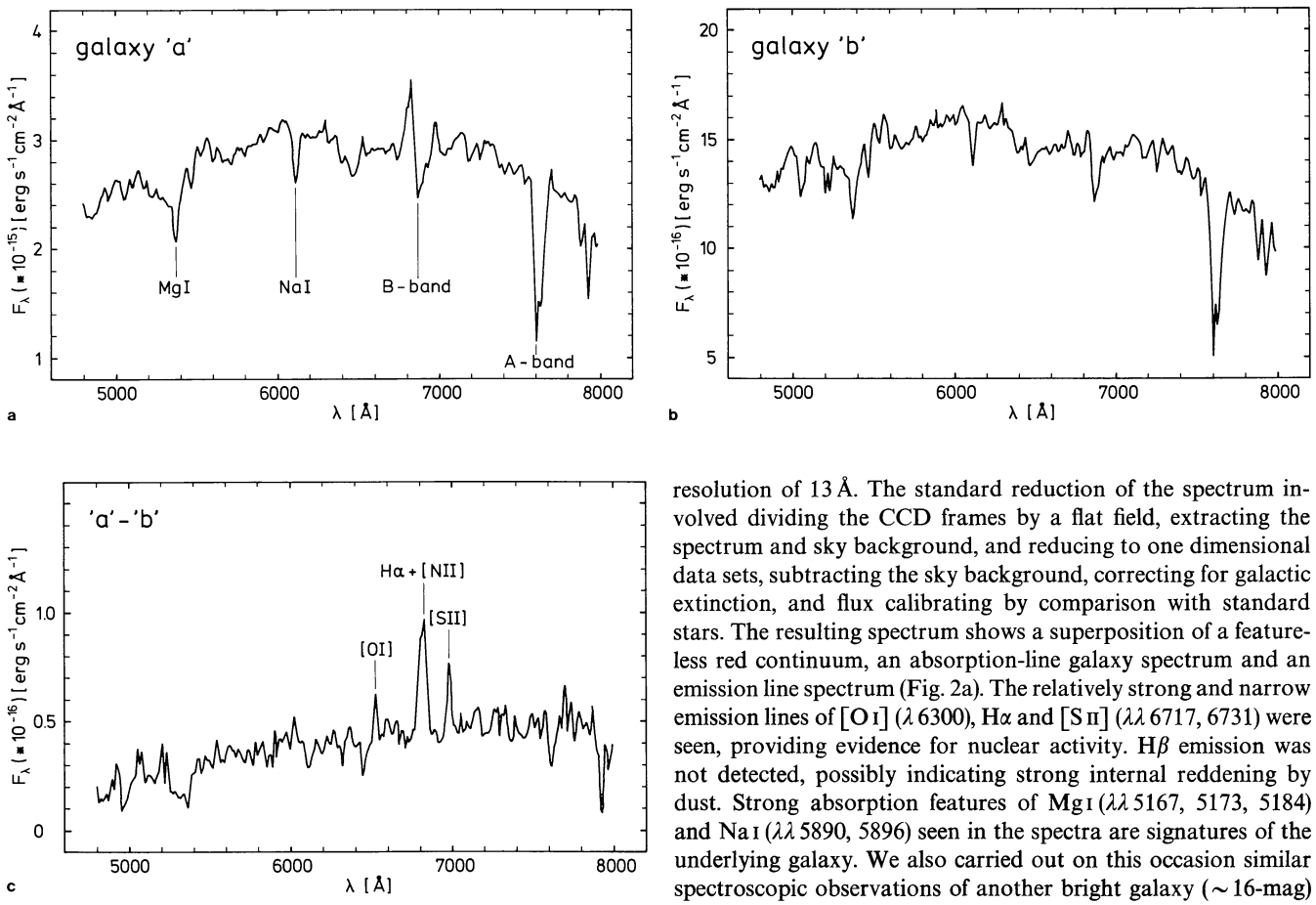

Fig. 2. a Optical low dispersion spectrum of galaxy 'a'; besides the atmospheric A – and B – bands strong absorption features of redshifted Mg I and Na I are detected as well as three emission lines; **b** same as in **a** for galaxy 'b' but no trace of any emission line; **c** spectrum **b** normalized at 6650 Å to the flux density level of galaxy 'a' and subtracted from **a**; the underlying red continuum and the emission lines in galaxy 'a' are apparent

spectrograph used was equipped with a RCA chip of 512 × 320 pixels detecting the spectrum between effective wavelengths of 4800 Å and 8000 Å. Two spectra with integration times of ~15 min each were taken through a long slit with a low spectral resolution of 13 Å. The standard reduction of the spectrum involved dividing the CCD frames by a flat field, extracting the spectrum and sky background, and reducing to one dimensional data sets, subtracting the sky background, correcting for galactic extinction, and flux calibrating by comparison with standard stars. The resulting spectrum shows a superposition of a featureless red continuum, an absorption-line galaxy spectrum and an emission line spectrum (Fig. 2a). The relatively strong and narrow emission lines of [O I] (λ 6300), Hα and [S II] (λλ 6717, 6731) were seen, providing evidence for nuclear activity. Hβ emission was not detected, possibly indicating strong internal reddening by dust. Strong absorption features of Mg I (λλ 5167, 5173, 5184) and Na I (λλ 5890, 5896) seen in the spectra are signatures of the underlying galaxy. We also carried out on this occasion similar spectroscopic observations of another bright galaxy (~16-mag) marked as 'b' in Fig. 1b. It is a spiral. The absorption features of Mg I and Na I detected in its spectrum are, within the errors, identical in redshift to that of the radio galaxy 'a' (Fig. 2b). As the absorption line spectra of the two underlying galaxies are similar we have normalized and subtracted the fainter from the brighter one, in order to reduce the effect of absorption features on the emission line strengths (Fig. 2c). Three emission lines mentioned above are clearly visible; the slope in the differential spectrum is probably due to a featureless red continuum from galaxy 'a', frequently seen in active galactic nuclei, rather than indicative of calibration problems. In Table 2 we list the observed

Table 2. The observed optical absorption and emission lines from the galaxies 'a' and 'b'

	Line	Observed λ_{peak}[Å]	Redshift	Relative flux
Galaxy 'a'	Mg I λ 5173	5370.2	0.0381	abs.
	Na I λ 5893	6116.7	0.0380	abs.
	[O I] λ 6300	6527.5	0.0361	59
	Hα + [N II] λ 6583	6827.3	0.0387	100
	[S II] λ 6717, 6731	6976.5	0.0376	31
			⟨0.038 ± 0.001⟩	
Galaxy 'b'	Mg I λ 5173	5372.9	0.0386	abs.
	Na I λ 5893	6117.6	0.0381	abs.
			⟨0.038 ± 0.001⟩	

wavelengths of identified absorption and emission line features along with their derived redshifts. The relative line strengths of the emission lines are also given; these were derived from the differential spectrum (Fig. 2c). The observed mean redshift of both galaxies is $z = 0.038 \pm 0.001$. These two galaxies and possibly several others seen in their vicinity may thus be members of a group or cluster of galaxies that seems to be stretched mainly towards north and east of the radio galaxy (Sect. 4; Fig. 1b).

4. Results

Although no unresolved radio component has been detected between the two radio lobes there is a strong indication that they are physically related to each other. Firstly, each radio lobe consists of a high-brightness 'hot spot' and a low-brightness extension ('tail') in the direction of the other lobe (Fig. 1). Secondly, a comparison of the 2.7 GHz map with the 1.4 GHz map (Fig. 1), after smoothing the former to the resolution of the latter, has revealed a large, systematic gradient of spectral index (α) along each lobe such that between the hot spot and the associated tail, α steepens by $\gtrsim 0.4$, as shown in Fig. 1d. Since such a pattern of spectral gradient and radio morphology is known to occur in lobes of powerful, extended double radio sources (e.g., Miley, 1980), we regard the pair of radio lobes shown in Fig. 1 as two components of a double radio source. The proposed identification of this source with the 15-mag elliptical galaxy 'a' (Figs. 1 and 2) is supported by the following considerations:

(i) The elliptical galaxy is located between the two radio lobes, close to the line joining them, and is clearly the brightest among the galaxies seen between the lobes.

(ii) Independent evidence for nuclear activity in this galaxy comes from its optical spectrum described in Sect. 3. Also, the internal dust-reddening inferred from the absence of Hβ line is known to be an indicator of radio loudness. (Disney et al., 1984; Sadler, 1982).

(iii) The elliptical appears to lie in a group of galaxies (Sects. 3 and 5) and is optically dominant among them. This circumstance would make it an almost exclusive candidate for strong radio emission (see Menon and Hickson, 1985).

The adoption of the active galaxy 'a' ($z = 0.038$) as the parent galaxy to the radio source implies a distance of 216 Mpc to the source. As seen from Fig. 1a, radio emission in each lobe extends significantly beyond the position of the peak. The largest separation between the lobes, measured at the third outermost contour is 40 arcmin, corresponding to a physical size of 2.5 Mpc. Thus, only 3C 236 is known to be significantly larger than this source (see Willis et al., 1974).

Here it may be noted that the other ellipticals seen between the two radio lobes are considerably fainter than the active galaxy 'a' and hence identification of the radio source with any of them would most probably imply even larger distance and physical size for the source. It may further be noted that no galaxy brighter than 18.5 mag is seen within the bright parts of the southern radio lobe (Fig. 1b). Thus, if indeed this lobe with an overall extent of $\gtrsim 15$ arcmin were an independent source, unrelated to the northern lobe, the inferred redshift of $z \gtrsim 0.2$ would imply for it a physical size of $\gtrsim 4$ Mpc. However, the evidence summarized above strongly favours the interpretation that the two lobes are physically related, with the identification for this double source being the 15-mag elliptical[1] marked 'a' in Fig. 1.

From the present single-dish measurements, the integrated flux densities at 1.4 and 2.7 GHz are found to be, respectively, 1.6 ± 0.15 Jy and 0.85 ± 0.05 Jy for the northern lobe and 1.2 ± 0.1 Jy and 0.77 ± 0.05 Jy for the sourthern lobe. The corresponding spectral indices are ($S_\nu \sim \nu^\alpha$) $\alpha = -1.0 \pm 0.2$ for the northern lobe and $\alpha = -0.7 \pm 0.2$ for the southern lobe. Combining these measurements with the integrated flux density of 60 ± 12 Jy at 85 MHz (Mills et al., 1960) gives $\alpha = -1.06 \pm 0.06$ for the whole source. We can use the 327 MHz synthesis map for estimation the spectral indices near the peaks of the two lobes where the effect of any 'missing flux' is unlikely to be significant. For this, the 327 MHz map was smoothed to the resolution of the 2.7 GHz map and a comparison of the two then gave $\alpha = -0.73 \pm 0.05$ and $\alpha = -0.74 \pm 0.05$ near the peaks of the northern and southern lobes, respectively.

Significant amount of linearly polarised emission is detected from both lobes at 2.7 GHz (Fig. 1d), the integrated polarised flux being 100 ± 10 mJy for the northern lobe and 50 ± 10 mJy for the southern lobe (or, 12% and 6.5%, respectively). At the peaks of the two lobes the percentage polarisation reaches 17% and 7.8%, respectively. Both lobes show a uniform distribution of the polarisation E vector, indicating a regular magnetic field structure. However, multifrequency radio observations are needed to account for any Faraday rotation.

5. Discussion

5.1. The structural asymmetry and the age of 0503-286

A noteworthy feature of this giant radio galaxy is the markedly asymmetric disposition of the two radio lobes relative to the parent galaxy (Fig. 1). Compared to the northern lobe, the southern lobe extends nearly twice as far from the nucleus (see below). Its 1 Mpc long tail runs along the axis joining the hot spot with the parent galaxy, suggesting that the beam energizing this lobe follows an essentially straight trajectory along the axis, shown with an arrow (Fig. 1a, b). The counter-beam to north probably also emerges from the nucleus parallel to this same axis. However, the northern lobe is offset from the axis towards west, as seen from Fig. 1a, b. While such an offset could have resulted from swinging of the beam, an alternative possibility emerges from an inspection of the optical field. The Palomar-Sky-Survey prints reveal a clustering of galaxy-like images around the parent galaxy 'a', mainly towards north and east of it. Down to ~17-mag, i.e., about 2-mag fainter than the radio galaxy 'a', such images can be clearly identified as galaxies and their approximate positions are plotted in Fig. 1b. One notices a concentration of the galaxies to the east of the northern lobe and a marked deficiency of them on the western side of the lobe. A similar deficiency of galaxies is found throughout the sector joining the nucleus with the southern lobe. Now, from Sect. 3, redshifts are presently available for just two of the galaxies, namely, 'a' and

[1] We learn that a central radio component associated with this galaxy has indeed been detected by C.R. Subrahmanya and R.W. Hunstead, at the Molonglo Observatory, who have independently discovered this giant radio galaxy (C.R. Subrahmanya, private communication).

Table 3. Comparison of the properties of giant radio galaxies

Name	Other name	Morph. class	Red-shift	Parameters for the entire source[a]								Parameters for the nuclear radio core				
				LAS arc	LLS Mpc	S^t_{408} Jy	P_{408} 10^{26} W/Hz	S^t_{5000} Jy	ψ deg	D	Ref. codes	S^c_{5000} Jy	β "arc	C_5 %	CF %	Ref. code
0055 + 300	NGC 315	FR-II	0.0167	58	1.7	9.6	0.1	2.13	10	2.1	1,2	0.62	1 × 3	29.1	6.5	2
0114 − 476		FR-II	0.146	9.6	2.0	10.4	10.4	2.31	19	1.4	3,4	–	–	–	–	
0136 + 396	4C 39.04	FR-II	0.2107	7.3	2.0	3.33	8.0	0.24	2	1.2	5	0.013	4 × 6	5.4	0.4	5
0211 − 479		FR-II	0.22	5.6	1.6	3.4	8.5	0.42	2	1.7	6,7	–	–	–	–	
0503 − 286		FR-II	0.038	40	2.5	10.5	0.7	0.85	16	1.9	8	–	–	–	–	
0744 + 559	DA 240	FR-II	0.0356	34	2.0	16.3	0.9	1.82	5	1.4	9,10	0.111	0.4	6.1	0.7	11
0945 + 734	4C 73.08	FR-II	0.0581	18.5	1.7	7.7	1.2	0.89	1	1.5	12					
1003 + 351	3C 236	FR-II	0.0988	39	5.8	10.9	4.9	2.93	2	1.6	9,10	1.5	1 × 2	51.2[b]	13.8[b]	13
1029 + 570	HB 13	FR-I	0.045	35	2.6	1.77	0.2	0.29	–	–	14,15	0.022[d]	4 × 4	7.6	1.2	14,15
1331-099		FR-II	0.081	12.9	1.6	6.7	2.0	≤1.5[c]	0	1.1	4,16	0.09	∼0.1	≥6	1.3	17
1549 + 202	3C 326	FR-II	0.0895	19.5	2.7	10.6	4.0	1.2	3	2.0	18	0.013	7 × 20	1.1	0.1	18
1637 + 826	NGC 6251	FR-II	0.023	52	2.0	5.51	0.1	1.46	16	2.5	19,20,21	0.9	∼1	61.6	16.3	20

[a] Computed for $H_0 = 50\,\mathrm{km\,s^{-1}\,Mpc^{-1}}$ and $q_0 = 0$

[b] A well known steep spectrum core. It contains a milli-arcsecond nucleus with $S_{5000} = 320 \pm 30$ mJy (Ref. 22), corresponding to $C_5 = 11\%$ and CF = 3%

[c] Extrapolated from 408 MHz, assuming $\alpha \leq -0.6$

[d] Extrapolated from the measured flux density at 2.7 GHz (Ref. 14) and $\alpha \overset{\text{core}}{\geq} -0.2$ (Ref. 15)

Reference codes: (1) Willis et al. (1981); (2) Bridle et al. (1979); (3) Danziger et al. (1983); (4) Bolton et al. (1964); (5) Hine (1979); (6) Danziger et al. (1978); (7) White et al. (1984); (8) present work; (9) Willis et al. (1974); (10) Strom et al. (1981); (11) van Breugel et al. (1983); (12) Mayer (1979); (13) Fomalont et al. (1979); (14) Masson (1979); (15) Andernach (1982); (16) Schlizzi and McAdam (1975); (17) Graham et al. (1981); (18) Willis and Strom (1978); (19) Waggett et al. (1977); (20) Jones et al. (1986); (21) Willis et al. (1982); (22) Barthel et al. (1985)

'b'. Even the perfect agreement between these two redshifts is no guarantee that the apparent clustering of galaxies seen in Fig. 1b indeed represents a physical association. But if this were to be borne out by future observations, an interesting evolutionary scenario for this giant radio galaxy can be visualised. According to this, both beams are ejected from the nucleus along the same axis (indicated by the arrow in Fig. 1b) in opposite directions, but the northern beam, unlike its southern counterpart, has to propagate through a relatively dense intergalactic medium associated with the 'cluster', which would slow its advance. Further, in this medium a large-scale decrease of gas density (and presumably of pressure too) towards west can be inferred from the apparent distribution of the galaxies, as mentioned above (Fig. 1b). The trajectory of the beam may then be bent towards west, along the pressure gradient (see Henriksen et al., 1981). Also, the radio lobe formed around this northern beam, if filled with lighter material, would be subjected to buoyancy and thus be drifting westward in the direction of lower ambient density. Since such a drift is expected to be subsonic, the velocity should be $< 10^3\,\mathrm{km\,s^{-1}}$ for a typical intra-cluster gas temperature of order 10^7 K. Such a drift velocity, in conjunction with the actually observed offset of the lobe from the axis, which amounts to 3–4 arcmin ($\gtrsim 200$ kpc; Fig. 1b) would suggest a minimum age of 10^8 yr for this giant radio galaxy.

5.2. Comparison of the properties of known giant radio galaxies (GRGs)

In Table 3, we have listed some radio parameters for a set of 12 radio galaxies known to have projected dimensions of ≥ 1.5 Mpc. In past, properties of GRGs have been compared using smaller samples (Waggett et al., 1977; Hine, 1979). A clear tendency for GRGs to occur outside rich clusters of galaxies has thus been noticed. The trend is maintained by the present, enlarged set of GRGs (Table 3). Another interesting result reported in the earlier studies relates to the equipartition energy densities inside the radio lobes of GRGs, which were found to be mostly within a factor of 2 of $10^{-13}\,\mathrm{erg\,cm^{-3}}$. But, as pointed out by these authors, observational selection could have led to the narrow dispersion. In the present work, we shall examine a different set of parameters, namely the radio luminosity at 408 MHz (P_{408}), the core-fraction (C_5 = fraction of the total flux contributed by the nuclear core at 5 GHz, or, CF = core flux at 5 GHz/total flux at 408 MHz), the 'asymmetry factor' (D = ratio of the separations of the outermost hot spots from the core) and the 'misalignment angle' (ψ = supplement of the angle subtended by the two outermost hot spots at the core). Values of these parameters for the GRGs are given in Table 3, together with the morphological classification (Fanaroff and Riley, 1974), total flux densities at 408 MHz and 5 GHz, core flux density at 5 GHz and the beamwidth (β) of the radio map used, the 'largest angular size' (LAS) and the corresponding linear size (LLS).

5.2.1. The radio morphology and luminosity

While the known GRGs are mostly edge-brightened classical double sources (Fanaroff-Riley class II, i.e., FR-II), examples of Z-shaped morphology (NGC 315) and of the 3C 31-type morphology (HB 13) are also present among them (Table 3). Since the latter two morphological types are frequently explained by invoking mechanisms such as the precession of the central engine or strong dissipation of the beam power, it is evident that a pair of highly 'efficient' and stable beams is not a pre-requisite for the formation of a giant source.

From Table 3, all the 12 GRGs fall within a rather narrow luminosity range from $10^{25} - 10^{27}\,\mathrm{W\,Hz^{-1}}$ at 408 MHz. While any less luminous GRGs would probably display an edge-darkened morphology (FR-I) due to which their sizes may have been underestimated, the lack of GRGs at high luminosities may be real. However, Baldwin (1982) has pointed out that in such luminous GRGs the accumulated synchrotron losses might quench the radio tails, rendering the physical association of the two lobes unestablished. Recently, such a GRG may indeed have been detected (Eales, 1985).

5.2.2. The misalignment and asymmetry of the double radio structure

From Table 3, the misalignment angle (ψ) for the GRGs, while usually remaining below $\sim 5°$, is found to range up to $\sim 20°$. Thus, the distribution of ψ for the GRGs is consistent with the median 'intrinsic' misalignment angle of $\sim 10°$ estimated by Macklin (1981) for a representative set of 3CR double sources of FR-II type, which are more luminous but statistically much smaller in size than the GRGs. For the same set of 3CR doubles, Macklin (1981) found the asymmetry parameter 'D' to be < 1.4 in half the cases. In contrast, only 2 of the 11 GRGs of FR-II type have $D < 1.4$. The tendency for GRGs to be unusually asymmetric has earlier been noted by Willis et al. (1981). In Sect. 5.1, the large asymmetry of the GRG 0503-286 ($D = 1.9$) was attributed to a stronger decceleration of its northern beam, caused by a relatively dense intergalactic medium, whose presence was inferred from the concentration of galaxies seen in the general direction of the northern lobe (Fig. 1b). To look for more evidence of this kind, we have examined the optical fields around the remaining substantially asymmetric ($D \geq 1.4$) and not too distant ($z < 0.2$) GRGs, following a procedure identical to that adopted for 0503-286 (Sect. 5.1). For 5 of the total 9 GRGs examined in this manner (namely, 0114-476, 0503-286, 3C 236, 3C 326 and NGC 6251) an obvious difference between the concentrations of optical galaxies was found between the two sides occupied by the two radio lobes. Interestingly, in all 5 cases the side with clearly lower concentration of galaxies coincides with the radio lobe that extends farther from the parent galaxy and also happens to be the weaker radio emitter than the other lobe. Details of this study which underlines the potential importance of the environment in explaining the large-scale asymmetry of double radio sources, will be published elsewhere.

5.2.3. The prominence of nuclear radio cores

The observed core-fractions of GRGs should be close to the intrinsic values, since the probability of a substantial Doppler boosting of the core emission due to any relativistic beaming is quite small in view of the fact that the projected dimensions of the GRGs are known to be the largest among radio galaxies and hence their radio axes are expected to be oriented away from the line of sight. In Table 3, core-fractions are given for the 8 GRGs for which maps are available at 5 GHz (or, alternatively at 2.7 GHz, together with an estimate of the core spectral index). The arcsecond resolution of these maps is adequate for distinguishing the cores from any adjacent radio features. Among these 8 GRGs, C_5 is found to exceed 10% in 3 cases and 5% in 7 cases.

The median value of C_5 for the entire set of 12 GRGs is thus $\gtrsim 5\%$ which is as high as the typical intrinsic core-fraction of 2–3% estimated for radio-loud quasars (Orr and Browne, 1982; Swarup et al., 1985) where nuclear activity is believed to be extraordinarily intense. In order to extend the comparison to the general population of radio galaxies resembling the GRGs in its range of redshift ($z < 0.5$) and median luminosity ($P_{408} \sim 10^{26}$ W Hz^{-1}), we have constructed a 'comparison sample' containing 93 radio galaxies, by merging the B2 'faint sample' and the '3CR sample' described by Feretti et al. (1984), each of which has been defined above a certain limiting optical magnitude and a limiting radio flux density at metre wavelengths. The radio axes of these galaxies, in contrast to the GRGs, are expected to be oriented randomly in the sky, because the comparison sample is defined at metre wavelengths where the emission is mainly contributed by 'unbeamed' radio lobes. From Fig. 3 of Feretti et al, we estimate for this sample a median value of CF (=core flux at 5 GHz/total flux at 408 MHz) in the range 0.2 to 1%, depending on what flux densities, between zero and the quoted upper limits, are assigned to the radio-undetected cores of many galaxies in the sample. Thus, the median value of CF for the radio galaxies in the comparison sample is probably close to 0.5% which is practically the same as that found for the set of GRGs (see Table 3). Thus, it appears that the nuclear radio cores are statistically as prominent among giant radio galaxies as they are among the general population of radio galaxies selected at a comparable level of radio luminosity but having much smaller physical size, on average. This is interesting, firstly because the giant radio sources are normally viewed as galaxies at a late stage of nuclear activity and, secondly because their nuclear radio emission is unlikely to have been boosted due to relativistic beaming, though the same could well be happening in the galaxies belonging to the comparison sample, as noted above.

To summarize, some of interesting features of the known giant radio galaxies, inferred from the present study are:

(i) a fairly narrow range in radio luminosity around an intermediate value of $P_{408} \sim 10^{26}$ W Hz^{-1}, (ii) an unusually asymmetric double radio structure, probably caused by an asymmetry of the environment about the parent galaxy, and (iii) a rather prominent nuclear radio emission. Searches for additional GRGs particularly at low frequencies are likelv to prove helpful in establishing the significance of these statistical trends which seem closely linked to the question of origin of such giant radio structures.

Acknowledgements. It is a pleasure to thank Drs. M.N. Joshi, H. Steppe, G. Swarup, W. Kundt and A.P. Rao for their valuable help and suggestions in course of this work, Mr. P.K. Manoharan provided enthusiastic support during the OSRT observations. We also gratefully acknowledge the ready access to the facilities at the Library Section of the Raman Research Institute.

References

Andernach, H.: 1982, Ph.D. thesis, Univ. of Bochum.

Baldwin, J.E.: 1982, in Extragalactic Radio Sources, Proc. IAU Symp **97**, eds. Heeschen, Wade, Reidel, Dordrecht, p. 21

Barthel, P.D., Schilizzi, R.T., Miley, G.K., Jägers, W.J., Strom, R.G.: 1985, *Astron. Astrophys.* **148**, 243

Bolton, J.G., Gardner, F.F., Mackey, M.B.: 1964, *Australian J. Phys.* **17**, 340

Bridle, A.H., Davis, M.M., Fomalont, E.B., Willis, A.G., Strom, R.G.: 1979, *Astrophys. J.* **228**, L9

Danziger, I.J., Goss, W.M., Frater, R.H.: 1978, *Monthly Notices Roy. Astron. Soc.* **184**, 341

Danziger, I.J., Goss, W.M.: 1983, *Monthly Notices Roy. Astron. Soc.* **202**, 703

Disney, M.J., Sparks, W.B., Wall, J.V.: 1984, *Monthly Notices Roy. Astron. Soc.* **206**, 899

Eales, S.A.: 1985, *Monthly Notices Roy. Astron. Soc.* **217**, 149

Fanaroff, B.L., Riley, J.M.: 1974, *Monthly Notices Roy. Astron. Soc.* **167**, 31p

Feretti, L., Giovannini, G., Gregorini, L., Parma, P., Zamorani, G.: 1984, *Astron. Astrophys* **139**, 55

Fomalont, E.B., Miley, G.K., Bridle, A.H.: 1979, *Astron. Astrophys.* **76**, 106

Graham, D.A., Weiler, K.W., Wielebinski, R.: 1981, *Astron. Astrophys.* **97**, 388

Haslam, C.G.T.: 1974, *Astron. Astrophys. Suppl.* **15**, 333

Henriksen, R.N., Vallee, J.P., Bridle, A.H.: 1981, *Astrophys. J.* **249**, 40

Hine, R.G.: 1979, *Monthly Notices Roy. Astron. Soc.* **189**, 527

Jones, D.L., et al.: 1986, *Astrophys. J.* **305**, 684

Large, M.I., Mills, B.Y., Little, A.G., Crawford, D.F., Sutton, J.M.: 1981, *Monthly Notices Roy. Astron. Soc.* **194**, 693

Macklin, J.T.: 1981, *Monthly Notices Roy. Astron. Soc.* **196**, 967

Masson, C.R.: 1979, *Monthly Notices Roy. Astron. Soc.* **187**, 253

Mayer, C.J.: 1979, *Monthly Notices Roy. Astron. Soc.* **186**, 99

Menon, T.K., Hickson, P.: 1985, *Astrophys. J.* **296**, 60

Miley, G.K.: 1980, *Ann. Rev. Astron. Astrophys.* **18**, 165

Mills, B.Y., Slee, O.B., Hill, E.R.: 1960, *Australian J. Phys.* **13**, 676

Orr, M.J.L., Browne, I.W.A.: 1982, *Monthly Notices Roy. Astron. Soc.* **200**, 1067

Sadler, E.M.: 1982, Ph.D. Thesis, The Australian Nat. Univ., Canberra.

Schilizzi, R.T., McAdam, W.B.: 1975, *Mem. Roy. Astron. Soc.* **79**, 1

Strom, R.G., Baker, J.R., Willis, A.G.: 1981, *Astron. Astrophys.* **100**, 220

Swarup, G.: 1984, *J. Astrophys. Astron.* **5**, 139

Swarup, G., Sinha, R.P., Hilldrup, K.: 1984, *Monthly Notices Roy. Astron. Soc.* **200**, 1067

Waggett, P.C., Warner, P.J., Baldwin, J.E.: 1977, *Monthly Notices Roy. Astron. Soc.* **181**, 465

White, G.L., McAdam, W.B., Jones, I.G.: 1984, *Proc. Astron. Soc. Aust.* **5**, 507

Willis, A.G., Strom, R.G., Wilson, A.S.: 1974, *Nature* **250**, 625

Willis, A.G., Strom, R.G.: 1978, *Astron. Astrophys.* **62**, 375

Willis, A.G., Strom, R.G., Bridle, A.H., Fomalont, E.B.: 1981, *Astron. Astrophys.* **95**, 250

Willis, A.G., Strom, R.G., Perley, R.A., Bridle, A.H.: 1982, in *Extragalactic Radio Sources, Proc.* IAU Symp **97**, eds. Heeschen, Wade, Reidel, Dordrecht, P 141

van Breugel, W., Heckman, T., Bridle, A.H., Butcher, H., Strom, R.G., Balick, B.: 1983, *Astrophys. J.* **275**, 61